Pergamon

Geochimica et Cosmochimica Acta, Vol. 67, No. 5, pp. 935–939, 2003

0016-7037/03 $30.00 + .00

PII S0016-7037(02)01222-X

A mechanism for the production of hydroxyl radical at surface defect sites on pyrite

MICHAEL J. BORDA,[1,*] ALICIA R. ELSETINOW,[2] DANIEL R. STRONGIN,[2] and MARTIN A. SCHOONEN[1]

[1]Department of Geosciences, E.S.S. Building, The State University of New York at Stony Brook, Stony Brook, NY 11794-2100, USA
[2]Department of Chemistry, Temple University, Philadelphia, PA 19122, USA

(*Received May* 24, 2002; *accepted in revised form September* 13, 2002)

Abstract—A previous contribution from our laboratory reported the formation of hydrogen peroxide (H_2O_2) upon addition of pyrite (FeS_2) to O_2-free water. It was hypothesized that a reaction between adsorbed H_2O and Fe(III), at a sulfur-deficient defect site, on the pyrite surface generates an adsorbed hydroxyl radical ($OH^{\bullet}$).

$$\equiv Fe(III) + H_2O_{(ads)} \rightarrow \equiv Fe(II) + OH^{\bullet}_{(ads)} + H^+$$

The combination of two $OH^{\bullet}$ then produces H_2O_2. In the present study, we show spectroscopic evidence consistent with the conversion of Fe(III) to Fe(II) at defect sites, the origin of H_2O_2 from H_2O, and the existence of $OH^{\bullet}$ in solution. To demonstrate the iron conversion at the surface, X-ray photoelectron spectroscopy (XPS) was employed. Using a novel mass spectrometry method, the production of H_2O_2 was evaluated. The aqueous concentration of $OH^{\bullet}$ was measured using a standard radical scavenger method. The formation of $OH^{\bullet}$ via the interaction of H_2O with the pyrite surface is consistent with several observations in earlier studies and clarifies a fundamental step in the oxidation mechanism of pyrite. *Copyright © 2003 Elsevier Science Ltd*

1. INTRODUCTION

It is the objective of this contribution to investigate the mechanism for pyrite-induced H_2O_2 production. This study reports the results of an experimental investigation of pyrite-induced H_2O_2 formation and tests the validity of two key assumptions in a proposed mechanism for the production of $OH^{\bullet}$ at defect sites at the pyrite surface. The proposed mechanism hypothesizes that the dissociation of H_2O, to form $OH^{\bullet}$ and H^+, occurs on nonstoichiometric Fe(III) sites on pyrite (Eqn. 1).

$$\equiv Fe(III) + H_2O_{(ads)} \rightarrow \equiv Fe(II) + OH^{\bullet}_{(ads)} + H^+ \quad (1)$$

The presence of nonstoichiometric Fe(III) and sulfur-deficient defect sites (i.e., S^{2-}) at the surface has been postulated and experimentally verified in prior studies (Guevremont et al., 1998a; Rosso et al., 1999a; Rosso et al., 1999b; Uhlig et al., 2001). In an earlier work, a mechanism for H_2O_2 production was proposed by Borda et al. (2001), based on the reactivity of Fe(III) sites toward H_2O. Briefly, Borda et al. (2001) reported aqueous concentrations of H_2O_2 when pyrite contacted H_2O, and showed that these concentrations increase as much as twofold from illumination with simulated sunlight. Additionally, experiments using pyrrhotite (FeS) and sphalerite (ZnS) showed no production of H_2O_2. In contrast, vaesite (NiS_2), which crystallizes in the pyrite structure, produces H_2O_2. The presence of the disulfide group (the characteristic group of the pyrite structure), in both minerals that produce H_2O_2, implicates the group to the reactivity. The full importance of $OH^{\bullet}$ in the pyrite system is not yet recognized, though the incorporation of $OH^{\bullet}$ into oxidation schemes is necessary and will develop an improved model of pyrite oxidation. Subsequently, the addition of $OH^{\bullet}$ in the pyrite oxidation system has implications for acid mine drainage studies and may pose a new consideration for potential abatement strategies.

2. RESEARCH STRATEGY

The goal of this research was to experimentally verify the proposed conversion of Fe(III) to Fe(II), the origin of H_2O_2 from H_2O, and the presence of $OH^{\bullet}$. X-ray photoelectron spectroscopy (XPS) was employed to experimentally test whether Fe(III) is converted to Fe(II) upon reaction with H_2O. Fe 2p core electron spectra were collected on a clean pyrite surface, on the same surface after generation of a high defect density, and finally on the same surface after exposure to H_2O.

To investigate the origin of H_2O_2, an innovative ultra-high vacuum (UHV) mass spectrometer experimental apparatus was designed. Experiments were run using synthesized pyrite prepared in our laboratory (for synthesis method see Borda et al., 2001). The apparatus allowed for in situ, timed mixing of aqueous solutions with potassium permanganate ($KMnO_4$) and successive introduction of headspace gas into the mass spectrometer. Solutions containing H_2O_2, when combined with $KMnO_4$, produced $O_{2(g)}$ as a product.

To verify the presence of $OH^{\bullet}$ in aqueous solution, a standard method based on the reaction of $OH^{\bullet}$ with benzene was used. The concentration of H_2O_2 in solution also was measured simultaneously using the same method reported in Borda et al. (2001).

3. RESEARCH METHODOLOGY

3.1. XPS Procedure

XPS results presented herein were obtained using an UHV chamber equipped with an integrated reaction cell. The integrated reaction cell allows for controlled exposure of the pyrite surface under environmentally relevant pressures, followed by

* Author to whom correspondence should be addressed (mike@pbisotopes.ess.sunysb.edu).

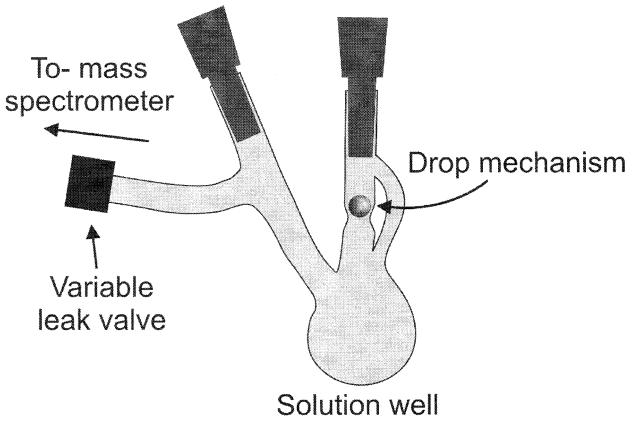

Fig. 1. Schematic diagram of reaction vessel experimental apparatus for mass spectrometry.

direct transfer into the UHV chamber for further analysis. This assembly was described in a previous report and permits samples to be analyzed under UHV conditions and transferred into environmentally relevant pressures without exposure to the laboratory environment (Guevremont et al., 1998b).

The pyrite sample used in the UHV study was a natural {100} surface originating from Lograno, Spain. The surface was approximately 1 $cm^2 \times 2$ mm, and the as grown surface was used. To clean the sample, 1000 eV He^+ ion bombardment was utilized to remove adventitious carbon and oxygen (Chaturvedi et al., 1996). After bombardment, the sample was removed into the reaction chamber, acid washed using 0.5 mol/L HCl, and rinsed with deoxygenated water to generate a {100} surface consistent with previously reported mechanically fractured surfaces (Elsetinow et al., 2000). These prior studies suggest that the acid-rinsed surface differs from the mechanically fractured surface largely because of the presence of additional polysulfide. The clean surface was reintroduced into the UHV chamber and analyzed using XPS. Fe 2p spectra were collected using Mg Kα (1253.6 eV) unmonochromatized radiation and a double-pass cylindrical mirror analyzer with a pass energy of 25 eV. After analysis of a clean, acid-washed surface, the sample was ion bombarded using 1000 eV He^+ to promote an increase in defect sites. The sample was then reanalyzed and transferred into the integrated cell for exposure to a droplet of deoxygenated DI H_2O for 1 h. After 1 h of exposure, the droplet was rinsed with 10 mL of deoxygenated DI H_2O and dried using a stream of $N_{2(g)}$. The sample was reinserted into UHV and analyzed.

3.2. Mass Spectrometry Procedure

The UHV mass spectrometer experiment required several steps. In the first step, a mineral slurry was prepared using a 4 g/L particle loading of hydrothermally synthesized, acid-washed pyrite and deoxygenated DI H_2O to produce 3 mL of slurry. In the second step, the slurry was filtered (0.45 μm nominal pore size) and placed in a glass vial. Filtrate was placed in a glass reaction vessel fitted behind a UHV variable leak valve (Fig. 1). Above the solution well, in the reaction vessel, a stainless steel ball bearing was seated and $KMnO_4$ crystals were placed above the drop mechanism. The reaction vessel was sealed and exposed to a series of three freeze-pump-thaw cycles to remove headspace gases. After subsequent cycles, the reaction vessel was open to the UHV chamber via the variable leak valve and a background spectrum of O_2 ($m/z = 32$) was obtained using a quadrupole mass spectrometer. When a consistent background was achieved, the drop mechanism was lifted using a magnet and $KMnO_4$ was allowed to fall into solution. The reaction sequence describing the production of O_2 from MnO_4^- and H_2O_2 is shown in Eqn. 2.

$$MnO_4^- + 3/2H_2O_2 + 2H^+ \rightarrow MnO_{2(s)} + 3/2O_{2(g)} + 2H_2O \quad (2)$$

Control experiments were run using DI H_2O, and prepared as outlined above but without pyrite. FeS slurry was also run.

3.3. $OH^\bullet$ Formation Analysis Procedure

The method for measuring the concentration of $OH^\bullet$ has been reported earlier (Faust and Allen, 1993). Briefly, the formation of $OH^\bullet$ can be monitored by analyzing for phenol produced from the $OH^\bullet$-mediated oxidation of benzene. In a glass reaction vessel, 400 mL of a 1-mM benzene solution was allowed to react with 1.51 g of hydrothermally synthesized pyrite. Phenol was analyzed using a standard spectrophotometer method (HACH™ method # 8047).

4. RESULTS

4.1. XPS Results

Pyrite {100} was acid washed and analyzed (Fig. 2A) with XPS. The Fe 2p spectrum shows a high intensity peak near 707 eV, consistent with Fe(II), the dominant iron state at the surface. In addition to this peak, lower intensity spectral weight is seen at 711 eV. This second, lower binding energy peak is consistent with Fe(III) at the surface. Actually, Fe(III) yields broad spectral weight due to multiplet splitting (Nesbitt and Muir, 1998). This spectral intensity is postulated to represent iron associated with a sulfur-deficient defect site.

After analysis of the acid-washed sample, it was bombarded with 1000 eV He^+ ions to induce a greater defect density. Figure 2B shows the effect of 30 min of ion bombardment on the iron component of pyrite. Data exhibited in the figures show that, after ion bombardment, there is a decrease of intensity near 707 eV (Fe(II)) and an increase at 711 eV (Fe(III)). While not shown here, the S 2p region shows an increase in spectral intensity below 162 eV that has been attributed to an increase in the surface concentration of S^{2-} (Guevremont et al., 1998b). Although the mechanism leading to the formation of Fe(III) and S^{2-} is unclear, it may be that ion bombardment removes some surface S^- from the S_2^{2-}, leading to transient S^- surface species (Elsetinow et al., 2001). This process may lead to neighboring iron being oxidized from Fe(II) to minority Fe(III) species, and the reduction of S^- to S^{2-}. This line of reasoning is similar to that proposed by Nesbitt et al. (1998) to explain the presence of Fe(III) and S^{2-} on fractured pyrite, although in this earlier work the disulfide bond was broken (formation of isolated S^{1-}) by the mechanical act of fracture.

Figure 2B shows that upon contact of the increased defect

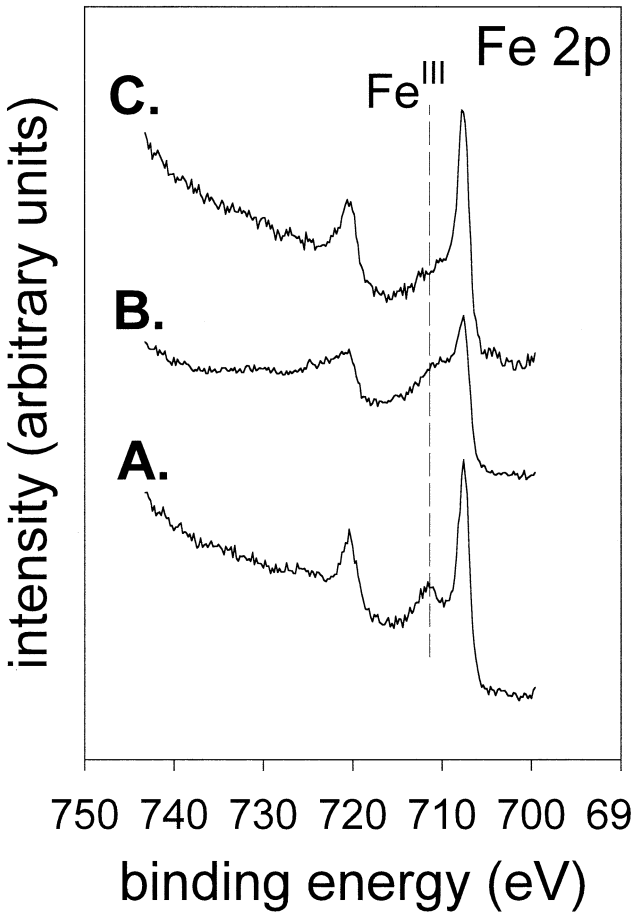

Fig. 2. XPS results showing Fe 2p spectra of (A) acid-washed pyrite (100), (B) pyrite (100) after 30 min 1000 eV He^{+} ion bombardment, and (C) reaction of pyrite (100) with deoxygenated DI H_2O for 1 h.

surface with deoxygenated DI H_2O for 1 h, a significant loss of intensity at 711 eV (Fe(III)) is seen along with a subsequent increase of intensity at 707 eV (Fe(II)) (Fig. 2C). These results, coupled with an extensive geochemical analysis of different pyrite types reported earlier (Borda et al., 2001), suggest that the conversion of Fe(III) to Fe(II) occurs on pyrite in the presence of H_2O.

4.2. Mass Spectrometry Results

The results of the mass spectrometry study are shown in Figure 3. The control spectrum shows the results of the experiment using DI H_2O. The arrow in the figure shows the time when $KMnO_4$ was dropped into solution. The pyrite spectrum shows the results of the experiment where the solution was a filtrate from a pyrite slurry. Immediately after addition of $KMnO_4$, there is a substantial increase in the O_2 entering the UHV chamber. A standard solution of 1 μM H_2O_2 was run to approximate the results of previous batch aqueous experiments (Borda et al., 2001). The spectrum has been multiplied by a factor of 3 to show a correlation with the pyrite spectrum. Finally, a spectrum was taken using the filtrate from a FeS slurry. The resulting spectrum is consistent with the control

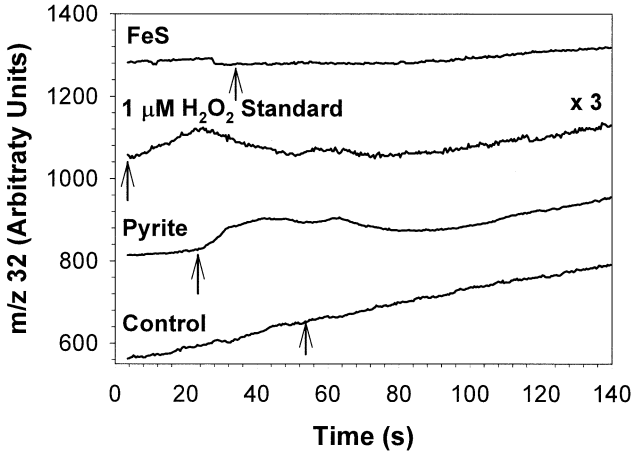

Fig. 3. Mass spectrometry results in m/z vs. time for control, pyrite, 1 μM H_2O_2 standard (x3), and FeS experiments. Arrows denote $KMnO_4$ drop.

spectrum showing no production of O_2. These results suggest that the mass spectrometry method is successful in measuring low concentrations of H_2O_2 and that pyrite is the only mineral tested that produces H_2O_2. There is also good correlation between the results of this study and concentrations in aqueous solution reported earlier (Borda et al., 2001). We are currently initiating a set of isotopic tracer experiments in an attempt to definitively determine the surface reaction responsible for the production of H_2O_2. With optimum conditions, isotopically labeled $H_2{}^{18}O$ could implicate the reactant in the formation mechanism (i.e., $Fe(III) + H_2{}^{18}O \rightarrow Fe(II) + {}^{18}OH^{\bullet} + H^{+}$) by analyzing for $^{36}O_2$ as a product in mass spectrometer experiments.

4.3. $OH^{\bullet}$ Formation Results

After 1 min of reaction time, the solution containing water, benzene, and pyrite had a 1 μM concentration of $OH^{\bullet}$. Simultaneously, H_2O_2 was measured and gave a concentration of 100 nM. These results verify the formation of $OH^{\bullet}$ in the pyrite–water system and are consistent with some of the $OH^{\bullet}$ rapidly forming H_2O_2.

5. DISCUSSION

In our earlier work, we hypothesized a mechanism for the production of H_2O_2 via the formation of $OH^{\bullet}$ at the surface as shown in Eqn. 1. Our results in this report are consistent with our previous hypothesis and allow us to interpret key observations in the literature from a new perspective.

Previous isotopic studies demonstrate that sulfate ($SO_4{}^{2-}$) produced during the oxidation of pyrite has an oxygen signature consistent with derivation from H_2O rather than O_2 (Reedy et al., 1991; Taylor et al., 1984a; Taylor et al., 1984b). Furthermore, studies find an anomalous burst of sulfate upon the initial contact of pyrite and water, despite thorough cleaning of samples before experimentation (Moses and Herman, 1991; Moses et al., 1987; Schoonen et al., 2000). Both theory and electrochemical experiments are consistent with Fe 3d dangling bonds dictating the sorption behavior of oxidants and control-

ling electron transfer on pyrite (Biegler and Swift, 1979; Rosso et al., 1999b). Most mechanistic pictures are, however, vague with regard to the reactions that lead to the oxidation of bulk S_2^{2-} or nonstoichiometric S^{2-}, other than to state the incorporation of oxygen from water in the sulfur oxide product. Our results suggest that H_2O_2 and $OH^\bullet$ may play a role in this sulfur oxidation chemistry. In particular, the initial production of sulfate may be the direct result of the reaction between nonstoichiometric S^{2-} and $OH^\bullet$. This notion has been experimentally supported by previous XPS work in our group showing clean {100} pyrite exposed to O_2-free water vapor immediately form sulfate. In these results, XPS S 2p peak intensity consistent with S^{2-} was seen to decrease as peak intensity consistent with sulfate appeared. The peak intensity associated with bulk S_2^{2-} stayed constant (Guevremont et al., 1998a).

The rate of pyrite oxidation has been shown to increase with exposure to simulated sunlight, and may in fact proceed via a different reaction mechanism when illuminated (Schoonen et al., 2000). Consistent with this finding are results that show an increase in H_2O_2 production with illumination (Borda et al., 2001). Capture of a photon promotes an electron from a nonbonding iron *d*-level to the conduction band of pyrite (Jaegermann and Tributsch, 1983). Hence, the formation of a hole (h^+) converts an Fe(II) to an Fe(III). If the hole migrates to the surface, it is capable of dissociating adsorbed H_2O and forming $OH^\bullet$. Some of the $OH^\bullet$ will combine and form H_2O_2. The formation of $OH^\bullet$ via this photochemical pathway may contribute to the presence of $OH^\bullet$ in surface waters affected by acid mine drainage (AMD) as reported in a study by Allen et al. (1996). In their study, illuminated water collected at an AMD site showed the formation and steady-state concentration of $OH^\bullet$. While $OH^\bullet$ may form via a number of photochemical pathways in these waters, we propose that photodissociation of pyrite-induced H_2O_2 may have been one of the sources. We are now conducting laboratory experiments to measure $OH^\bullet$ and H_2O_2 concentrations during a batch oxidation experiment to evaluate this notion.

Though this is the first experimental verification of $OH^\bullet$ in the pyrite–water system, the presence of $OH^\bullet$ in reaction sequences used to describe pyrite oxidation is not new. Moses et al. (1987) suggested a mechanism for the oxidation of pyrite by a solvated Fe^{3+} complex involving the dissociation of a water of hydration to form $OH^\bullet$. They then suggest a step-wise oxidation of the disulfide group by $OH^\bullet$.

6. SUMMARY AND IMPLICATIONS

The results of this study suggest that the defect structure of the pyrite surface is capable of dissociating H_2O to form $OH^\bullet$, supporting an earlier hypothesis. The fate of $OH^\bullet$ appears to be twofold. First, a fraction of $OH^\bullet$ combines to form H_2O_2 in solution and is therefore sequestered in a significantly less reactive form. Second, we hypothesize that a fraction of $OH^\bullet$ reacts to oxidize sulfur at the pyrite surface consistent with previous observations. This initial reactivity appears to precede further pyrite oxidation by other oxidants, such as molecular O_2. Overall, this new reaction scheme unifies previously diverse observations about the initial reactivity of the pyrite surface and offers a new insight into reactive species produced therein.

In studying the mechanisms that produce AMD and developing abatement strategies, it is necessary to consider the impact of $OH^\bullet$ on the stability of adsorbed inhibitors. In the field of astrobiology, pyrite-induced $OH^\bullet$ represents a potentially important species. For example, one may have to consider the stability of organic molecules in the presence of $OH^\bullet$ on an early Earth, and the implications this may have for prebiotic synthesis.

In environmental applications, pyrite has been identified as a suitable redox site provider for enhancing the transfer of electrons in pollutant degradation procedures (Arienzo, 1999; Weerasooriya and Dharmasena, 2001). With a band gap of approximately 1 eV for bulk pyrite (Xu and Schoonen, 2000) and 2.2 eV for 2-nm nano-pyrite (Wilcoxon et al., 1996), it has become a candidate material for solar energy conversion and for this same reason may be important as a substrate in photo-assisted contaminant degradation systems. In all of these cases, it may be the existence, and reactivity, of $OH^\bullet$ that plays a crucial role. Further investigation into this problem is unquestionably warranted.

Acknowledgments—M.A.S. and D.R.S. greatly appreciate support from the Department of Energy, Basic Energy Sciences from grants DEFG029ER14633 and DEFG0296ER14644, respectively. Dave Plasket is thanked for his extraordinary glass blowing talent and his satire. We also thank two anonymous reviewers and Associate Editor Udo Becker for comments and suggestions that improved the quality of this manuscript.

Associate editor: U. Becker

REFERENCES

Allen J. M., Lucas S., and Allen S. K. (1996) Formation of hydroxyl radical in illuminated surface waters contaminated with acidic mine drainage. *Environ. Toxicol. Chem.* **15**(2), 107–113.

Arienzo M. (1999) Oxidizing 2,4,6-trinitrotoluene with pyrite-H_2O_2 suspensions. *Chemosphere* **39**(10), 1629–1638.

Biegler T. and Swift D. A. (1979) Anodic behaviour of pyrite in acid solutions. *Electrochim. Acta* **24,** 415–420.

Borda M., Elsetinow A., Schoonen M., and Strongin D. (2001) Pyrite-induced hydrogen peroxide formation as a driving force in the evolution of photosynthetic organisms on an early Earth. *Astrobiology* **1**(3), 283–288.

Chaturvedi S., Katz R., Guevremont J., Schoonen M. A. A., and Strongin D. R. (1996) XPS and LEED study of a single-crystal surface of pyrite. *Am. Mineral.* **81,** 261–264.

Elsetinow A. R., Guevremont J. M., Strongin D. R., and Schoonen M. A. A. (2000) Oxidation of {111} and {100} planes of pyrite: Effects of surface atomic structure and preparation method. *Am. Mineral.* **85,** 623–626.

Elsetinow A. R., Schoonen M. A. A., and Strongin D. R. (2001) Aqueous geochemical and surface science: Investigation of the effect of phosphate on pyrite oxidation. *Environ. Sci. Technol.* **35**(11), 2252–2257.

Faust B. C. and Allen J. M. (1993) Aqueous-phase photochemical formation of hydroxyl radical in authentic cloudwaters and fogwaters. *Environ. Sci. Technol.* **27**(6), 1221–1224.

Guevremont J., Bebié J., Elsetinow A. R., Strongin D. R., and Schoonen M. A. A. (1998a) Reactivity of the (100) plane of pyrite in oxidizing gaseous and aqueous environments: Effects of surface imperfections. *Environ. Sci. Technol.* **32,** 3743–3748.

Guevremont J. M., Elsetinow A. R., Strongin D. R., Bebié J., and Schoonen M. A. A. (1998b) Structure sensitivity of pyrite oxidation: Comparison of the (100) and (111) planes. *Am. Mineral.* **83,** 1353–1356.

Jaegermann W. and Tributsch H. (1983) Photoelectrochemical reactions of FeS_2(pyrite) with H_2O and reducing agents. *J. Appl. Electrochem.* **13,** 743–750.

Moses C. O. and Herman J. S. (1991) Pyrite oxidation at circumneutral pH. *Geochim. Cosmochim. Acta* **55,** 471–482.

Moses C. O., Nordstrom D. K., Herman J. S., and Mills A. L. (1987) Aqueous pyrite oxidation by dissolved oxygen and by ferric iron. *Geochim. Cosmochim. Acta* **51,** 1561–1567.

Nesbitt H. W., Bancroft G. M., Pratt A. R., and Scaini M. J. (1998) Sulfur and iron surface states on fractured pyrite surfaces. *Am. Mineral.* **83**(9–10), 1067–1076.

Nesbitt H. W. and Muir I. J. (1998) Oxidation states and speciation of secondary products on pyrite and arsenopyrite reacted with mine waters and air. *Mineral. Petrol.* **62,** 123–144.

Reedy B. J., Beattie J. K., and Lowson R. T. (1991) A vibrational spectroscopic ^{18}O tracer study of pyrite oxidation. *Geochim. Cosmochim. Acta* **55,** 1609–1614.

Rosso K. M., Becker U., and Hochella M. F. (1999a) Atomically resolved electronic structure of pyrite {100} surfaces: An experimental and theoretical investigation with implications for reactivity. *Am. Mineral.* **84,** 1535–1548.

Rosso K. M., Becker U., and Hochella M. F. J. (1999b) The interaction of pyrite {100} surfaces with O_2 and H_2O: Fundamental oxidation mechanisms. *Am. Mineral.* **84,** 1549–1561.

Schoonen M. A. A., Elsetinow A., Borda M., and Strongin D. R. (2000). Effect of temperature and illumination on pyrite oxidation between pH 2 and 6. *Geochem. Trans.* **4**.

Taylor B. E., Wheeler M. C., and Nordstrom D. K. (1984a) Isotope composition of sulphate in acid mine drainage as measure of bacterial oxidation. *Nature* **308,** 538–542.

Taylor B. E., Wheeler M. C., and Nordstrom D. K. (1984b) Stable isotope geochemistry of acid mine drainage: Experimental oxidation of pyrite. *Geochim. Cosmochim. Acta* **48,** 2669–2678.

Uhlig I., Szargan R., Nesbitt H. W., and Laajalehto K. (2001) Surface states and reactivity of pyrite and marcasite. *Appl. Surface Sci.* **179**(1–4), 222–229.

Weerasooriya R. and Dharmasena B. (2001) Pyrite-assisted degradation of trichloroethene (TCE). *Chemosphere* **42**(4), 389–396.

Wilcoxon J. P., Newcomer P. P., and Samara G. A. (1996) Strong quantum confinement effects in semiconductors: FeS_2 nanoclusters. *Solid State Communica.* **98**(6), 581–585.

Xu Y. and Schoonen M. A. A. (2000) The absolute energy position of conduction and valence bands of selected semiconducting minerals. *Am. Mineral.* **85,** 543–556.